Behavioral/Systems/Cognitive

Deep Brain Stimulation of the Subthalamic Nucleus Alters the Cortical Profile of Response Inhibition in the Beta Frequency Band: A Scalp EEG Study in Parkinson's Disease

Nicole Swann,[1,2] **Howard Poizner,**[2,3] **Melissa Houser,**[4] **Sherrie Gould,**[4] **Ian Greenhouse,**[1] **Weidong Cai,**[1] **Jon Strunk,**[1] **Jobi George,**[1] **and Adam R. Aron**[1,2]

[1]Department of Psychology, [2]Neuroscience Graduate Program, and [3]Institute for Neural Computation, University of California San Diego, La Jolla, California 92093, and [4]Scripps Green Hospital, La Jolla, California 92037

Stopping an initiated response could be implemented by a fronto-basal-ganglia circuit, including the right inferior frontal cortex (rIFC) and the subthalamic nucleus (STN). Intracranial recording studies in humans reveal an increase in beta-band power (~16–20 Hz) within the rIFC and STN when a response is stopped. This suggests that the beta-band could be important for communication in this network. If this is the case, then altering one region should affect the electrophysiological response at the other. We addressed this hypothesis by recording scalp EEG during a stop task while modulating STN activity with deep brain stimulation. We studied 15 human patients with Parkinson's disease and 15 matched healthy control subjects. Behaviorally, patients OFF stimulation were slower than controls to stop their response. Moreover, stopping speed was improved for ON compared to OFF stimulation. For scalp EEG, there was greater beta power, around the time of stopping, for patients ON compared to OFF stimulation. This effect was stronger over the right compared to left frontal cortex, consistent with the putative right lateralization of the stopping network. Thus, deep brain stimulation of the STN improved behavioral stopping performance and increased the beta-band response over the right frontal cortex. These results complement other evidence for a structurally connected functional circuit between right frontal cortex and the basal ganglia. The results also suggest that deep brain stimulation of the STN may improve task performance by increasing the fidelity of information transfer within a fronto-basal-ganglia circuit.

Introduction

Imagine you are about to step into the street. Suddenly a car runs a light. Immediately, you stop your impending movement to avoid being struck. Experimentally, stopping action can be measured with tasks such as the stop signal and Go/NoGo. Converging evidence, from lesion, fMRI, and transcranial magnetic stimulation studies, points to a specific brain system for stopping, including the right inferior frontal cortex (rIFC), the pre-supplementary motor area, and the subthalamic nucleus (STN) (for review, see Aron et al., 2007b; Chambers et al., 2009; Chika-zoe, 2010) (and see recent studies by Isoda and Hikosaka, 2008; Neubert et al., 2010). Moreover, these regions are connected via

white matter tracts (Inase et al., 1999; Johansen-Berg et al., 2004; Aron et al., 2007a; Ford et al., 2010; Forstmann et al., 2010).

Recent evidence provides clues about the nature of neural communication within this network. One study recorded intra-cranial EEG from the rIFC during a stop signal task and found enhancement in the beta frequency band (~16 Hz) for successful versus failed stop trials (Swann et al., 2009) (also see Marco-Pallarés et al., 2008). Another study recorded local field potentials from the STN in patients and reported an enhancement in the beta-band for NoGo compared to Go trials (Kühn et al., 2004). These studies suggest that the putative structurally connected, functional network for stopping could operate in the beta-band. Here we tested this idea by recording scalp EEG while modulating STN activity using deep brain stimulation (DBS) in Parkinson's disease (PD) patients.

Each patient performed a stop signal task, with STN stimulation either ON or OFF. Matched healthy controls were also studied. The stop signal task was used because of the aforementioned evidence relating it to a prefrontal–STN circuit and to the beta-band, because it provides a sensitive and stable behavioral measure of stopping performance—the stop signal reaction time (SSRT)—and because the task has already been used in PD. Patients off medication have worse stopping performance (longer SSRT) than controls (Gauggel et al., 2004), while patients ON STN stimulation have faster SSRT than OFF (van den Wilden-berg et al., 2006) (but see Ray et al., 2009). We thus predicted that

Table 1. Demographic and rating scale measures

	PD patients—mean (SD)	Controls—mean (SD)
Age (years)	64.4 (6.8)	66.4 (8.0)
Sex	12 males/1 female	11 males/3 females
Handedness	13 right/0 left/0 ambidex.	12 right/1 left/1 ambidex.
MMSE	29.2 (0.6)	29.6 (0.6)
NAART	41.1 (10.3)	46.4 (7.1)
Beck*	8.9 (6.9)	3.4 (2.7)
UPDRS**		
OFF Stim.	50.8 (7.5)	N/A
ON Stim.	36.8 (6.9)	N/A

MMSE, Mini-Mental Status Exam; NAART, North American Adult Reading Test; Beck, Beck Depression Inventory. *$t_{(25)}$ = 2.76, p = 0.011; **$t_{(12)}$ = 9.63, $p \ll 0.0001$ for ON stimulation versus OFF stimulation; higher values reflect more impaired performance. Maximum score is 108.

SSRT would be longer for patients OFF STN stimulation than for healthy controls, and that SSRT would be improved with stimulation ON.

We performed time–frequency analyses of the EEG data. Based on prior intracranial and scalp EEG studies (Marco-Pallarés et al., 2008; Swann et al., 2009), we predicted that stopping would be associated with an enhancement in the beta-band for frontal electrodes, and we predicted, especially, that this beta enhancement would be different for ON versus OFF DBS. Thus, we aimed to show that STN stimulation modulates task-related beta-band activity as measured at the scalp. Such a finding would provide evidence for the hypothesis that beta-band information transfer underlies the putative fronto-STN network for stopping. We also performed standard event-related potential analyses. We predicted differences in the N2/P3 complex for OFF versus controls and for OFF versus ON. This was based on prior studies with this task, which have shown differences in these components for successful versus failed stop trials (Pliszka et al., 2000; Kok et al., 2004; Ramautar et al., 2006; Schmajuk et al., 2006; Liotti et al., 2007) (reviewed by Folstein and Van Petten, 2008).

Materials and Methods

Participants and demographics. We studied 15 patients with Parkinson's disease (PD) who had bilaterally implanted stimulating electrodes in the STN, and 15 matched controls. Two patients were excluded from analysis because mean RT was too long (>1 s) and because of too-frequent omissions on go trials (one patient had only 57% correct go trials for a session and the other patient had only 45% correct go trials). One control subject was excluded due to excessive head movement artifacts in the EEG, which were uncorrectable in subsequent processing. Therefore, the data presented are from 13 patients and 14 controls.

The PD patients were clinically evaluated by a trained movement disorders specialist (M.H.) and were found to have moderate PD [stages II to III of the Hoehn and Yahr scale (Hoehn and Yahr, 1967)]. All patients had clinically typical PD and were responsive to STN DBS in our study [see below; mean Unified Parkinson's Disease Rating Scale (UPDRS) (Goetz et al., 1995), score of 36.8 for ON and 50.8 for OFF stimulation ($t_{(12)}$ = 9.63, $p < 0.001$)]. The patients and controls were well matched on age, gender, and handedness, as well as on the Mini-Mental Status Exam (a screen for dementia) and the North American Reading Test (a test of IQ) (all p values >0.05) (see Table 1). Although the patients did score higher on the Beck Depression Inventory ($t_{(25)}$ = 2.76, p = 0.011) compared to controls, the mean score of 8.9 in PD patients reflects a mild, nonclinically relevant, level of depression that is typical for PD status.

The patients took their anti-parkinsonian medication as normal (see Table 2 for medications and dosages, DBS stimulation settings, individual patient UPDRS scores, and other clinical details). However, doses of such medications were markedly reduced from the levels used before STN DBS surgery. All participants were free from significant upper limb or trunk arthritis or pain, and were without any significant neurological or psychiatric disease, except for Parkinson's disease in the PD patients.

The patients were recruited from the Scripps Clinic in La Jolla, California, and the control participants were recruited from the local community. All participants provided written informed consent according to an Institutional Review Board Protocol of the University of California, San Diego.

Procedure. Each patient and control visited the laboratory once. The patients completed two EEG sessions—one ON their prescribed bilateral stimulation settings and one with the stimulator turned OFF bilaterally. The order of stimulation sessions was counterbalanced across patients. When patients were ON stimulation first, the procedure was as follows: informed consent was provided, followed by completion of rating scales (Mini-Mental Status Exam, North American Adult Reading test, Beck Depression Inventory and handedness test), UPDRS #1, EEG setup and task explanation, EEG session #1, stimulator switched OFF, 1 h break, EEG session #2, UPDRS #2, and stimulator returned to ON position. When patients were OFF stimulation first, the procedure was as follows: informed consent was provided, followed by completion of rating scales, UPDRS #1 (patients were in the ON state as usual), stimulator turned OFF, EEG setup and task explanation, UPDRS #2, EEG session #1, stimulator switched ON, 1 h break, and EEG session #2. Regardless of which session was first, we ensured that at least 1 h elapsed after the stimulator was turned OFF, before both the OFF UPDRS and OFF EEG session, to ensure that the majority of the stimulator effects had expired (Temperli et al., 2003).

For controls, the visit involved consenting, rating scales, and one session of EEG.

The stop signal task. Stimuli were presented on a 22 inch monitor placed 25 inches from the participant. Two button boxes, one for each hand, were used for response collection. The button boxes were placed in a vertical position allowing a lateral movement of the index finger. This movement engages the first dorsal interosseus muscle, which is optimal for electromyography.

Each trial began with a white fixation cross centered on a black background. After 500 ms, a white square appeared, equiprobably to either the right or the left of the cross (Go signal). Subjects responded accordingly using a button press with either their left or right hand within a limited hold time of 1.5 s. On a minority of trials (33%), the white square turned red [Stop signal (SS)] after a variable delay (Fig. 1A). This stop signal delay (SSD) between the Go signal and the Stop signal was varied using a dynamic tracking (staircase) procedure. The delay was made smaller when the subject failed to stop, and longer with success (50 ms intervals) to achieve a 50% stopping rate and to keep the task challenging at all times. The SSD values were selected from four independently moving staircases (two for each response direction) (for details, see Aron and Poldrack, 2006). There were five blocks of 96 trials each. The patients performed two sessions (ON and OFF), and controls performed one session.

EEG recordings. EEG data were recorded using a 64 + 8 channel Biosemi ActiveTwo system (Biosemi Instrumentation) sampled at 512 Hz. Extra electrodes were placed on both mastoids, below and lateral to the right eye, and over the first dorsal interosseous muscles of each hand (one on belly and one on tendon) to record electromyography. For the analyses that follow, the button presses were sufficient and the electromyography is not further discussed.

Behavioral analysis. The following measures were calculated: Go RT (average reaction time on correct go trials); failed stop RT (reaction time on stop trials where the participant failed to stop); percent go discrimination errors (percentage of go trials where participants responded with the wrong button box); percent go omission errors (%) (percentage of go trials where no response was made); probability of stopping overall (percentage of stop trials where stopping was successful); probability of stopping after convergence [probability of stopping after the SSD staircases had reached convergence, i.e., p(stop) ≈ 50%]; overall SSD (average stop signal delay over all staircases for the whole experiment); convergence SSD (average stop signal delay over all staircases after the point where convergence was reached); and SSRT (stop signal reaction time).

SSRT was calculated using the convergence method (Logan et al., 1997; Verbruggen and Logan, 2009a). For each subject, SSRT is calculated as mean Go RT minus grand average SSD (Fig. 1B). The grand average SSD is the average of SSD values in each of four staircases after

Table 2. Patient clinical characteristics

Patient ID	Age/gender/handedness	Disease duration (years)	Years since surgery	Medications	Left treatment setting (contact #, voltage, pulse width/Hz)	Right treatment setting (contact #, voltage, pulse width/Hz)	UPDRS (OFF/ON)
ST01	60/M/R	15	4	(1) Comtan 200 mg bid (2) Sinemet 25/100 half 5×/d (3) Requip 2 mg 5×/d (4) Azilect 1 mg (5) Clonazepam 0.5 mg	Case+ 1−, 2.4, 60/185	Case+ 5−, 3.3, 60/185	63/44
ST02	68/M/R	14	2	(1) Sinemet 25/100, qid (2) Stalevo 150 mg, qid (3) Requip XL 8 mg 1.5 tabs (4) Azilect 1 mg	Case+ 1−, 3.1, 60/185	Case+ 5−, 2.9, 60/185	42/31
ST03	58/F/R	8	0.33	(1) Sinemet CR 25/100 tid (2) Xanax 0.5 mg up to tid (3) Artane 1 mg bid	Case+ 1−, 0.6, 60/130	Case+ 5−, 3.0, 150/130	54/33
ST04	73/M/R	6	0.6	(1) Sinemet 25/100 bid	Case+ 2−, 2.5, 90/160	Case+ 5−, 1.7, 90/160	57/42
ST05	61/M/R	11	0.67	(1) Stalevo 100 mg bid (2) Mirapex 1 mg qd	Case+ 1−, 0.8, 90/130	Case+ 4−, 2.1, 90/130	42/30
ST06	53/M/R	15	2	(1) Sinemet 50 mg tid	Case+ 1−, 2.5, 60/185	Case+ 5−, 2.4, 60/185	47/35
ST07	72/M/R	4	0.6	(1) Azilect 1 mg (2) Parcopa 100 mg tid	Case+ 0−, 1.0, 60/180	Case+ (5,4)−, 2.1, 90/180	56/34
ST08	73/M/R	12	3	(1) Sinemet 100 mg tid (2) Sinemet 100 mg hs (3) Amantadine 100 mg bid (4) Requip 4 mg tid (5) Clonazepam 1 mg	Case+ 1−, 2.6, 60/160	Case+ 5−, 2.6, 60/160	49/45
ST09	69/M/R	11	1	(1) Stalevo 100 mg qid (2) Eldepryl 5 mg bid (3) Requip XL8 bid (4) Requip 1 mg	3+ 1−, 2.9, 60/80	7+ (5,6)−, 2.5, 60/80	58/40
ST10	66/M/R	5	0.75	(1) Stalevo 100 mg tid (2) Requip XL 8 mg (3) Azilect 0.5 mg	Case+ 1−, 2.6, 60/130	Case+ 4−, 1.5, 60/130	37/21
ST11	60/M/R	10	0.75	(1) Sinemet 25/100 bid (2) Mirapex 0.5 mg bid (3) Azilect 1 mg	Case+ 1−, 3.3, 90/160	7+ 5−, 3.5, 90/160	53/40
ST12	68/M/R	18	2	(1) Namenda 10 mg bid (2) Sinemet 25/100 tid (3) Mirapex 1.5 mg tid (4) Comtan 200 mg tid (5) Exelon 9.5 mg	Case+ 1−, 2.5, 60/185	Case+ 5−, 2.5, 60/185	48/41
ST13	56/M/R	10	0.28	(1) Requip 8 mg qd (2) Azilect 1 mg (3) Stalevo 50 mg tid	3+ 2−, 2.4, 60/160	7+ 5−, 2.2, 60/160	55/43

qd, Once a day; bid, twice a day; tid, three times a day; qid, four times a day; hs, at bedtime.

convergence to a stopping rate of ∼50%. SSRT was also computed using the integration method (Verbruggen and Logan, 2009b). However, results did not differ between these two methods, so only the convergence results are reported. Paired *t* tests were used to compare ON versus OFF stimulation. Unpaired *t* tests were used to compare controls versus ON and controls versus OFF.

EEG preprocessing. The data were preprocessed using a combination of EEGlab (Delorme and Makeig, 2004) (http://www.sccn.ucsd.edu/eeglab) and custom Matlab scripts. The data were first re-referenced to the mastoids (right and left). Next, the mean of each channel (over the whole dataset) was removed and an additional 0.05 Hz high-pass filter was applied to reduce low-frequency drift. The DBS artifact was very high frequency (usually 130–180 Hz), so most of the artifact could be removed using low-pass filtering. Accordingly, a 50 Hz low-pass filter was applied to all data (ON stimulation, OFF stimulation, and controls). The filtering steps in both cases used the EEGlab "eegfilt" function, a two-way FIR filter. Eye movement and blink artifacts were removed using independent component analysis (Jung et al., 2000). Components that corresponded to eye blinks/movements were identified using a published technique that compares favorably with other artifact rejection techniques, even for patient populations (Jung et al., 2000)—for each subject/

session, we identified at least one component that corresponded to ocular artifacts. Visual inspection confirmed both that the correct component was selected for each individual and that no detected residual blinks remained in the data.

EEG analysis. ERP and time–frequency analysis were performed with custom Matlab scripts. For each of these methods, we focused on data from a right frontal "region of interest." This was defined as a group of three right frontal electrodes (F6, F8, FC6) based on a previous scalp EEG study that showed right-lateralized stopping-related responses with the same task (Schmajuk et al., 2006). Here we analyzed all stop trials together, i.e., including both successful and failed stop trials. Our rationale was to increase statistical power. Note that the prerogative to test patients on the same day in two EEG sessions (ON vs OFF stimulation) meant that the length of each session had to be restricted (5 blocks of 96 trials, with 33% of these being stop trials). This is the lower bound of trial numbers needed for EEG analysis (Luck, 2005). Hence, averaging over both successful and failed stop trials was important.

ERP analysis involved the following steps: further low-pass filtering at 30 Hz; averaging across trials; aligning stop trials to the onset of the stop signal; subtraction, from the stop trials, of an average prestimulus baseline (−200 to 0 ms relative to the stop signal); averaging of the resulting

ERP across the three channels in the right frontal electrode cluster (F6, F8, FC6); and comparison of the ERPs for the three different conditions (ON, OFF, and controls).

Time–frequency analysis involved the following steps: raw data were filtered into individual frequencies using a wavelet method; data were epoched and averaged relative to the stop signal; an intertrial interval baseline was removed; an optional *z*-scoring procedure was performed (see below); data were averaged across three channels in the right frontal electrode cluster; averages were taken across subjects; and finally *t* tests were performed to compare conditions. These steps are now discussed in more detail.

First, a previously published method was used to filter each subject's raw EEG signal into 32 separate frequencies between 2 and 32 Hz (Canolty et al., 2007; Swann et al., 2009) In brief, first a fast Fourier transform was performed on the whole dataset. This output was then multiplied by 32 Gaussians centered at the selected frequencies. The SD of each Gaussian varied depending on the selected center frequency (to allow for higher temporal resolution in the higher frequencies). An inverse Fourier transform was then applied to the filtered data to produce analytic signal values. This technique is analogous to a Gabor wavelet transform performed in the frequency domain for computational efficacy, and yields an analytic amplitude signal for each of the 32 specified frequencies (Canolty et al., 2007). The absolute value of this number represents the amplitude of the signal, or "power." Second, data were extracted for stop trials, aligned so that time 0 was the stop signal, and averaged across trials for each frequency individually.

Third, an average baseline for each frequency (corresponding to -1500 to -1000 ms relative to the stop signal, falling in the intertrial interval) was subtracted from the trial data. Fourth, data were averaged across the three channels in the right frontal electrode cluster. Fifth, data were averaged across subjects separately for the three conditions: ON stimulation, OFF stimulation, and controls. Finally, a point-by-point paired *t* test was performed across subjects to test the idea that beta power around the time of stopping might differ for ON compared to OFF stimulation. An unpaired *t* test was performed for both ON and OFF compared to controls. One-sample *t* tests compared to zero were used to examine stop trials compared to baseline for each group separately.

An auxiliary analysis was also performed to see whether the results differed if the data were normalized before averaging across subjects. For this step, done after baseline correction, but before averaging across channels (between steps three and four), *z*-scores were derived from the averaged epoched data, using a permutation method (Canolty et al., 2007; Swann et al., 2009). These *z*-scored values were then used for the remainder of the calculations. This method did not produce substantially different results, so only the non-*z*-scored results are reported.

Results

Behavioral results

SSRT was significantly longer for PD patients OFF stimulation than for healthy controls ($t_{(25)} = 2.8$, $p < 0.01$) (Fig. 2A), consistent with an earlier study (Gauggel et al., 2004). SSRT was significantly speeded when patients were ON compared to OFF stimulation ($t_{(12)} = 2.4$, $p < 0.05$), similar to previous results (van den Wildenberg et al., 2006). SSRT was longer for ON versus controls, but this was not a significant difference ($t_{(25)} = 1.6$, $p =$
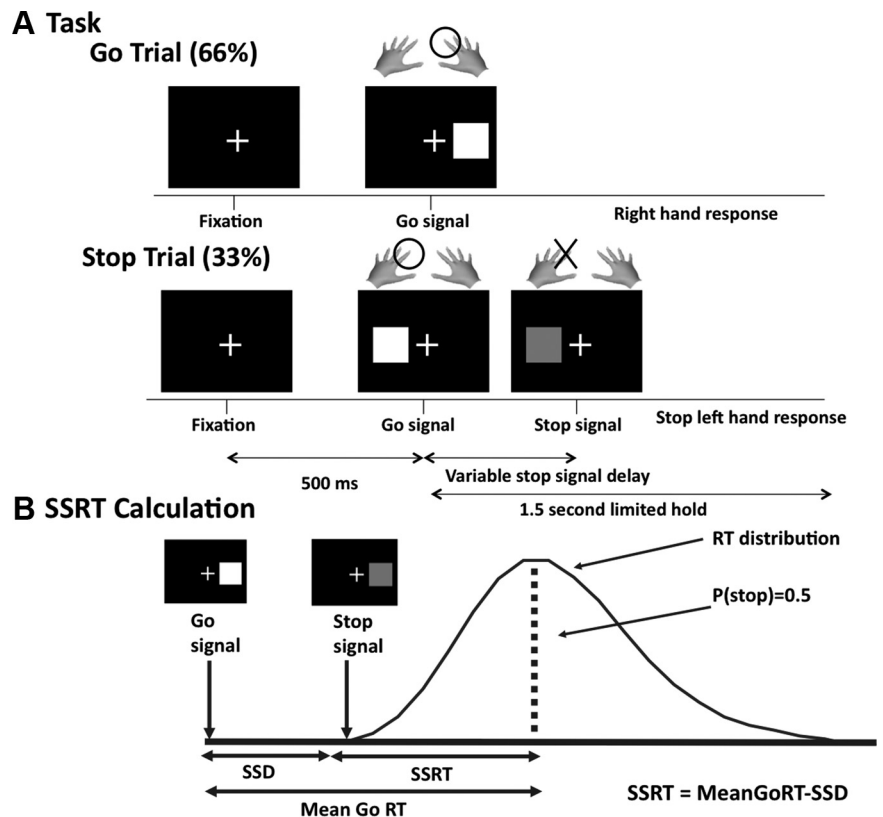

Figure 1. Stop signal task. **A**, Each trial began with a fixation cross, followed 500 ms later by the appearance of a white square (Go signal). The square appeared to either the left or the right of the fixation cross, requiring a response from the corresponding hand. Stop trials were identical to go trials, except they were less likely (33% of trials) and the white square turned red after a variable delay (stop signal delay). **B**, Schematic illustrating the way in which SSRT is calculated. The SSD is varied dynamically to yield a probability of stopping, *p*(stop), of $\sim$0.5. Assuming the Go and Stop processes race each other independently, this 50% point will correspond to the mean of the Go distribution. SSRT can then be calculated as MeanGoRT $-$ SSD.

0.12) (Fig. 2A). Similar results obtained even for nonparametric, Wilcoxon, tests.

A scatter plot of SSRT for ON versus OFF stimulation showed two interesting features (Fig. 2B). First, there was a significant correlation across subjects (Pearson's $r = 0.74$, $p < 0.01$). This illustrates that SSRT estimation was highly reliable. Second, it was apparent that every patient, except one, showed an improvement of SSRT with stimulation. Thus the ON versus OFF effect was highly robust.

Strikingly, these between-group SSRT differences were evident even while Go RT was not different ($t_{(12)} = 0.93$, $p = 0.37$) (Fig. 2C,D) and nor was any other measure (all *p* values >0.05) (Table 3). Thus, the effect of stimulation was specific to the stopping process.

We performed several auxiliary analyses. SSRT did not differ depending on which hand was stopped ($p > 0.1$ for all left vs right hand comparisons for each of ON stimulation, OFF stimulation, and control groups). Moreover, the slower SSRT for ON versus OFF was unlikely due to fatigue: in an ANOVA with the factors of session order (i.e., ON then OFF vs OFF then ON) and STN DBS status (i.e., ON vs OFF), there was no interaction ($F_{(1,11)} = 2.3$, $p = 0.16$).

EEG—time–frequency results

ON versus OFF stimulation was compared to examine the predicted stopping-related beta power difference (Marco-Pallarés et al., 2008; Swann et al., 2009). Importantly, there was significantly greater beta power around the time of stopping for ON compared
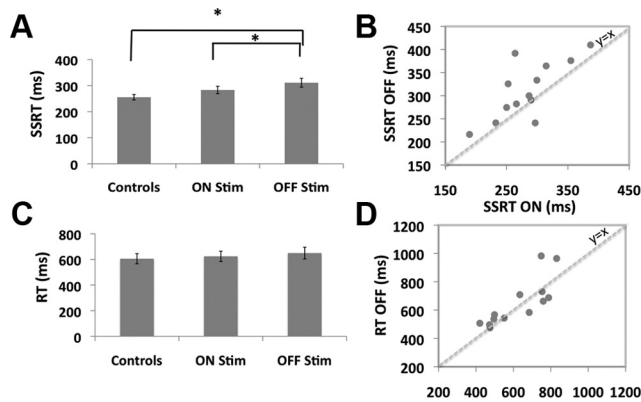
Figure 2. Behavioral results. *A*, SSRTs were significantly longer for patients OFF stimulation compared to ON stimulation and for patients OFF stimulation compared to controls (both $p <$ 0.05). *B*, SSRTs for individual patients. SSRT estimation was reliable since there was a strong correlation ($r = 0.74, p < 0.01$). The speeding of SSRT for ON versus OFF stimulation was also robust since every patient bar one improves. *C*, Go RT was not different. *D*, Go RT for individual patients. There was a strong correlation between ON and OFF ($r = 0.81, p < 0.01$); however, STN DBS did not affect Go RT consistently.

Table 3. Stop signal task behavioral performance

		Patients	
	Controls	ON Stim.	OFF Stim.
Go RT (ms)	606 (143)	624 (144)	650 (166)
Failed stop RT (ms)	522 (127)	550 (127)	554 (137)
Go discrimination error (%)	0.3 (0.5)	2.5 (4.1)	1.9 (2.9)
Go omission error (%)	0.6 (1.1)	3.4 (7.3)	2.8 (5.6)
Prob. stop overall (%)	54.5 (4.8)	53.8 (3.9)	54.2 (6.1)
Prob. stop after converge (%)	51.2 (6.4)	50.5 (2.6)	51.1 (3.7)
Overall SSD (ms)	330 (127)	322 (135)	313 (137)
Convergence SSD	350 (145)	341 (155)	338 (180)
SSRT*	256 (39)	283 (51)	311 (62)

Go RT, Mean correct go reaction time; Failed stop RT, mean reaction time on failed stop trials; Go discrimination error, percentage of discrimination errors on go trials; Go omission error, percentage of omission errors on go trials; Prob. stop overall, probability of stopping on stop trials overall; Prob. stop after converge, probability of stopping on stop trials after convergence; Overall SSD, mean stop signal delay overall; Convergence SSD, stop signal delay after convergence; SSRT, stop signal reaction time. *ON versus OFF: $t_{(12)} = 2.4, p = 0.033$; controls versus ON: $t_{(25)} = 1.6$, $p = 0.12$; controls versus OFF: $t_{(25)} = 2.8, p = 0.009$.

to OFF ($t_{(12)} > 3.05, p < 0.01$) (Fig. 3A) (a similar result was obtained with a Wilcoxon test). Because it is possible that this result relates to the use of different baselines for ON versus OFF, we also performed the analysis on data that did not have the baseline removed. A similar beta power difference (in the same direction) was found—therefore, baseline differences did not drive this key effect (Fig. 3B). Differences between controls and patients were examined, but were not significant, probably because of reduced power for the between-group as opposed to within-group comparison.

To examine the spatial specificity of the ON versus OFF difference, we performed the same analysis for a left frontal electrode cluster (F5, F7, FC7). There was no significant difference for ON versus OFF for beta power ($p > 0.05$) (Fig. 4A). However, other differences seen in the right frontal analysis (e.g., an early theta effect) were still apparent. This suggests that it is specifically the beta effect that was right lateralized. A paired t test showed that the right hemisphere electrode cluster had significantly greater beta power for the ON versus OFF comparison around the time of stopping compared to the left hemisphere ($t_{(12)} > 2.18, p < 0.05$) (Fig. 4D).

To further examine the specificity of this effect to the right frontal cortex, we also examined a frontal midline electrode clus-
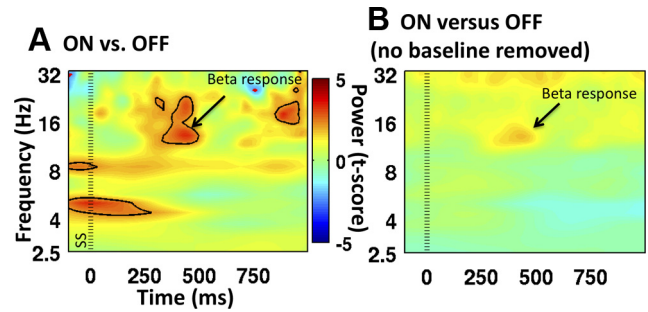

Figure 3. Time–frequency plots for stop trials for ON versus OFF stimulation. *A*, Significantly greater beta power ($\sim$16 Hz) for patients ON compared to OFF stimulation. Both conditions are first normalized to their own baselines before subtraction. *B*, The effect in *A* is still visible even when the comparison is made between ON versus OFF without first applying a baseline correction. Power is expressed with color as a t-score. Zero milliseconds was the time of the stop signal, SS (indicated with the standard dotted line). Power changes that are significant at $p < 0.05$ are encircled with either a black line (for ON $>$ OFF) or a red line (for OFF $>$ ON).

ter (Fz, F1, and F2), and two parietal clusters, in the left and right hemispheres (P5, P7, and CP5 and P6, P8, and CP6, respectively). In these three clusters there was also a beta difference between ON and OFF (potentially due to volume conduction), but for each cluster the beta effect was smaller than for the right frontal cluster, and this was a significant difference when comparing right frontal and left parietal clusters ($t_{(12)} > 2.18, p < 0.05$). Overall, while we are mindful that strong conclusions about cortical sources cannot be made from scalp recordings, our results suggest the beta effect is largest over the right hemisphere and perhaps especially over the right frontal region (cf. Swann et al., 2009). Note that while it was specifically beta changes that were observed for stopping when comparing ON versus OFF, the ON versus OFF comparison for go trials did not show such a specific effect. Instead there were general power differences across many frequencies (see Notes).

Each condition (ON stimulation, OFF stimulation, and controls) was separately examined relative to baseline to see what drove the observed difference between ON and OFF, and to address the prediction of increased beta power soon after the stop signal (Marco-Pallarés et al., 2008; Swann et al., 2009). For controls, there was a beta increase above baseline starting around 200 ms after the stop signal, a time consistent with this group's SSRT (Fig. 5C). This effect was small, not quite reaching significance with the point-by-point test. A similar pattern was observed for patients ON stimulation (at a slightly longer latency, perhaps reflecting prolonged SSRT) (Fig. 5A). However, no such pattern was observed for patients OFF stimulation (Fig. 5B).

To visualize how the beta increase might be related to SSRT, beta power was averaged over 15–17 Hz (Swann et al., 2009), and plotted over time, with a prestimulus baseline of −500 to 0 relative to the stop signal (Fig. 5D). Notably, the beta power increase began before SSRT. Moreover, the controls had the earliest beta peak and the shortest SSRT, whereas both were delayed for patients ON stimulation. OFF stimulation patients exhibited disorganized beta activity with no clear peak.

EEG—event-related potentials
ERPs were calculated for each group (patients ON and OFF stimulation and controls) to examine changes in the N2/P3 complex associated with response inhibition (Ramautar et al., 2006; Schmajuk et al., 2006; Liotti et al., 2007; Folstein and Van Petten,
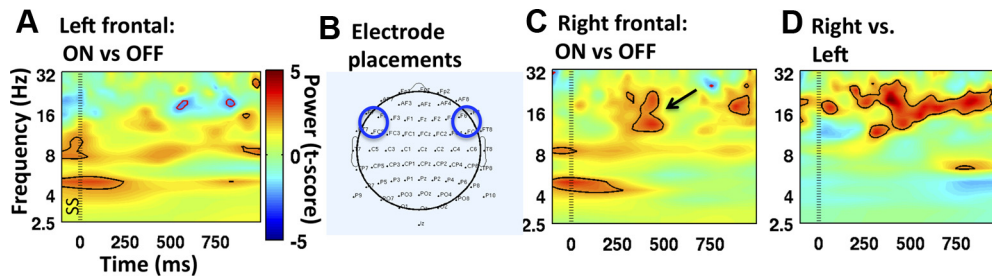
Figure 4. The beta increase of ON versus OFF is stronger over the right hemisphere than the left. **A**, Time–frequency plot of stop trials ON versus OFF for a left frontal ROI. The beta difference around the time of SSRT is not significant. **B**, Left and right frontal ROIs. The left electrode cluster includes F5, F7, and FC5, and the right one includes F6, F8, and FC6. **C**, The plot is the same comparison as Figure 4 A, but with data from a right frontal ROI. Note the significant beta difference around the time of stopping. Power is expressed in color as a *t*-score. Zero milliseconds was the time of the SS (indicated with the standard dotted line). Power changes significant at *p* < 0.05 are encircled with either a black line (for ON > OFF) or a red line (for OFF > ON). Note that this figure is identical to Figure 3*A*. **D**, Time–frequency plot comparing the ON versus OFF stimulation effects for stop trials in the right frontal ROI versus the left frontal ROI. Power differences are expressed in color as a *t*-score. Power differences significant at *p* < 0.05 are encircled in black (for right > left) or red (left > right). The beta power around the time of stopping is significantly greater in the right frontal ROI.
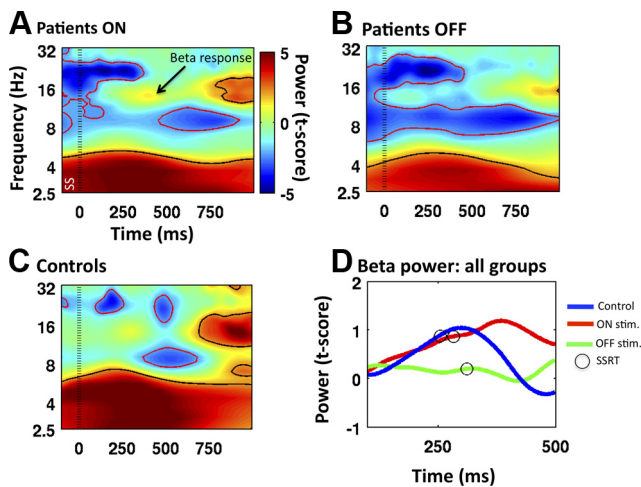

Figure 5. Time–frequency plots for stop trials. **A–C**, Power expressed with color as a *t*-score is plotted for patients ON stimulation (**A**), OFF stimulation (**B**), and controls (**C**). Note the predicted response in the beta-band for controls and patients ON stimulation. Zero milliseconds was the time of the SS (indicated with the standard dotted line). Power changes that are significant at *p* < 0.05 are encircled with either a black line (for increases above baseline) or a red line (for decreases below baseline). **D**, Average beta power from 15 to 17 Hz using a pre-stimulus baseline (−500 to 0). For controls, there is an increase in beta power before SSRT elapses. Patients ON stimulation show a slightly later increase consistent with a longer SSRT. There is no discernable beta increase for patients OFF stimulation.

2008). While ERPs for these components were present, the comparison between conditions was not easily made because the patients had overall reduced amplitude of all ERPs compared to controls (i.e., for all components, not merely stopping-related ones). Comparisons of ON to OFF stimulation did not reveal significant differences for the N2/P3 complex. This probably relates to the low trial numbers. Consequently, we do not further discuss ERPs and instead focus on the time–frequency results. Note that it is not unusual to have different findings for ERP compared to time–frequency analysis since ERPs reflect only phase-locked activity and primarily the very low frequencies, while time–frequency analyses capture non-phase-locked activity as well as higher frequencies (such as beta).

Discussion

Consistent with prior reports, we show that PD patients OFF stimulation were worse at stopping motor responses than healthy controls and that this deficit was ameliorated by STN DBS. The

EEG showed an increase in beta-band power for ON versus OFF stimulation, which was greater over the right frontal region than the left. These results support the hypothesis that stopping a motor response involves communication within a fronto-basal-ganglia circuit in the beta frequency band.

Our behavioral finding that SSRT is affected by STN DBS supports imaging studies in humans (Aron and Poldrack, 2006; Aron et al., 2007b; Li et al., 2008), lesion studies in rodents (Eagle et al., 2008), and neurophysiological recordings in primates (Isoda and Hikosaka, 2008), all pointing to STN as a key node for stopping. The improvement in stopping for ON versus OFF STN DBS agrees with one prior STN DBS study (van den Wildenberg et al., 2006), but not with another (Ray et al., 2009) (however, the latter study used all unilaterally implanted patients—which may account for the difference). Thus, our findings affirm that bilateral STN stimulation, at treatment-prescribed settings, shortens SSRT to levels near healthy age-matched controls. These behavioral findings set the stage for a comparison of EEG beta power.

Critically, we observed a greater beta response for stop trials for ON versus OFF stimulation over the right frontal electrode cluster but not over the left frontal cluster. Moreover, the right frontal effect was significantly greater than the left frontal one, consistent with a putative right-lateralized network for inhibitory control (Garavan et al., 1999, 2006; Konishi et al., 1999; Aron et al., 2003; Rieger et al., 2003; Rubia et al., 2003; Chikazoe, 2010). These results support our hypothesis of a structurally connected functional network between frontal cortex and STN that operates in the beta-band (Kühn et al., 2004; Swann et al., 2009). The results also speak to the therapeutic mechanism by which STN DBS may restore behavioral control. We speculate that STN DBS reduces the pathologically high beta synchrony between the basal ganglia and cortex so that task-related communication is facilitated. The reasoning is as follows. In untreated PD, there is pathologically high resting beta activity (reviewed by Brown and Williams, 2005; Brown, 2007; Hammond et al., 2007; Garcia-Munoz et al., 2010). This activity is associated with bradykinesia and rigidity (Kühn et al., 2006, 2009), and is reduced by dopamine replacement therapy and STN DBS (Kühn et al., 2006, 2008; Wingeier et al., 2006). Thus, STN DBS may improve symptoms by reducing the basal ganglia's pathologically high resting beta synchrony (Kühn et al., 2008; Garcia-Munoz et al., 2010). By contrast, we show that ON versus OFF STN DBS leads to increased cortical beta activity during task performance. Thus, the distinction between resting activity and task activity is key. If STN

DBS leads to normal levels of background or resting beta oscillatory activity, then this could "free up" neurons to allow a resumption of task-related beta coupling, as may be needed for stopping (Garcia-Munoz et al., 2010). Thus, STN DBS may have its behavioral benefit by improving the fidelity of information transfer in cortico-basal-ganglia circuits (Brown, 2007).

Our hypothesis was that the beta increase relates to implementation of the stopping process via cortical-STN communication. If so, the beta increase should occur before the end of the stopping process, i.e., before SSRT. Although the beta increase clearly began before SSRT had elapsed (Fig. 5D), the peak beta difference tended to fall after the average SSRT, later than expected. Several considerations bear on this. First, assuming the beta increase reflects cortical-STN communication via long-distance coupling, then it is not clear that this communication should abruptly terminate after stopping is implemented. Indeed, an intracranial EEG study showed a beta increase soon after the stop signal, which was maintained for a few hundred milliseconds, such that it peaked shortly after SSRT (Swann et al., 2009). If this sustained pattern occurred in the current study, then one would expect the observed pattern of an initial increase in beta after the stop signal with the peak occurring after SSRT (Fig. 5A). Second, SSRT is a single estimate that is derived for each individual, yet, on a trial-by-trial basis, the speed of stopping doubtless varies. Thus variability in the time at which stopping happens for an individual subject could produce some "spread" in the beta response. Third, there is variability in SSRT between individuals, further increasing spread of the beta response. Fourth, time–frequency analysis introduces some temporal imprecision (the SD for 16 Hz is 67 ms). Notwithstanding these considerations, it is clearly the case that the increase begins before SSRT elapses.

A paradoxical aspect of the current findings is that STN DBS improves stopping (and see van den Wildenberg et al., 2006), while, in rare cases, STN DBS leads to the opposite of good stopping, i.e., impulsive behavior such as hypomania and hypersexuality (Kulisevsky et al., 2002; Appleby et al., 2007). However, these rare cases may result from inadvertent stimulation of the ventral (limbic) territory of the STN (Mallet et al., 2007), or of adjacent structures or fibers of passage. If this is the case, it explains why such symptoms are rare and why they were not observed in our patients, since typical therapeutic stimulation sites are in the dorsal (sensorimotor) territory of the STN (reviewed by Kuncel and Grill, 2004).

There were several limitations to this study. First, some effects (e.g., ERPs and within-condition comparisons of stop vs baseline) were weak. This likely relates to the small trial number. EEG studies normally involve several hundred trials for averaging. Yet we needed to keep the trial number relatively low to keep the length short enough for PD patients to perform both ON and OFF sessions on the same day without fatigue. (The same-day sessions were important to reduce variability.) Notwithstanding the low trial number, there were clear-cut behavioral differences and EEG differences for ON versus OFF. A second limitation that flows from the first is that we could not compare successful and failed stop trials as prior studies have done (Ramautar et al., 2006; Schmajuk et al., 2006; Marco-Pallarés et al., 2008). Instead, because of low trial number, we grouped together all stop trials. Although comparisons of successful and failed stopping would be interesting, the fact that we analyzed all stop trials together does not impugn our finding that beta-band activity was greater for ON versus OFF stimulation. Third, we did not include an OFF medication condition—instead the patients were tested on their

normal medications. Since PD medications have been shown to alter beta activity in the STN (Kühn et al., 2006), it would also be interesting to examine beta activity during stopping in patients who are OFF medication. Fourth, because we recorded scalp EEG, we cannot make specific claims about which cortical area(s) underlie the beta increase, except to say they are evidently stronger in the right hemisphere than the left. Fifth, our study falls short of tightly linking the beta power increase to SSRT or the success/failure of stopping. However, other studies have demonstrated this relationship. Greater beta power for successful compared to failed stopping has been reported for scalp EEG (Marco-Pallarés et al., 2008) and for intracranial EEG from the rIFC specifically (Swann et al., 2009). We note that, even considering these studies, it is unclear which precise cognitive function relates to the beta increase. It is likely that rIFC is important for both attentional detection (Hampshire et al., 2010; Sharp et al., 2010) and implementing inhibitory control (Aron et al., 2004; Neubert et al., 2010), and these functions may be dissociable to different IFC subregions (Chikazoe, 2010; Verbruggen et al., 2010). While it is possible that attentional detection could involve coupling with the basal ganglia in the beta-band, the evidence is stronger that the beta-band is important for motor function, such as inhibitory control. For example, entraining beta synchronizations in motor cortex leads to slowed movement (Pogosyan et al., 2009), and performing NoGo trials leads to increased beta activity in the STN (Kühn et al., 2004). Future work is required to investigate whether the increase in cortical beta relates to attentional detection, inhibitory control, or both. However, our contribution here is to show that behavioral stopping has its counterpart in an increase in beta-band amplitude from right frontal electrodes, and that this is modulated by STN DBS.

In summary, we have shown that STN stimulation improves stopping behaviorally and modulates scalp recorded beta activity at a time consistent with the stopping process. Together with earlier results (Marco-Pallarés et al., 2008; Swann et al., 2009), these findings support the hypothesis that there is a structurally connected functional network between the cortex and STN that operates in the beta-band. In addition, these results provide insight into the mechanism by which STN stimulation improves action control. Specifically, they suggest that the therapy works by increasing the fidelity of information transfer in cortico-basal-ganglia networks during task performance.

Notes

References

Appleby BS, Duggan PS, Regenberg A, Rabins PV (2007) Psychiatric and neuropsychiatric adverse events associated with deep brain stimulation: a meta-analysis of ten years' experience. Mov Disord 22:1722–1728.

Aron AR, Poldrack RA (2006) Cortical and subcortical contributions to Stop signal response inhibition: role of the subthalamic nucleus. J Neurosci 26:2424–2433.

Aron AR, Fletcher PC, Bullmore ET, Sahakian BJ, Robbins TW (2003) Stop-signal inhibition disrupted by damage to right inferior frontal gyrus in humans. Nat Neurosci 6:115–116.

Aron AR, Robbins TW, Poldrack RA (2004) Inhibition and the right inferior frontal cortex. Trends Cogn Sci 8:170–177.

Aron AR, Behrens TE, Smith S, Frank MJ, Poldrack RA (2007a) Triangulating a cognitive control network using diffusion-weighted magnetic resonance imaging (MRI) and functional MRI. J Neurosci 27:3743–3752.

Aron AR, Durston S, Eagle DM, Logan GD, Stinear CM, Stuphorn V (2007b) Converging evidence for a fronto-basal-ganglia network for inhibitory control of action and cognition. J Neurosci 27:11860–11864.

Brown P (2007) Abnormal oscillatory synchronisation in the motor system leads to impaired movement. Curr Opin Neurobiol 17:656–664.

Brown P, Williams D (2005) Basal ganglia local field potential activity: character and functional significance in the human. Clin Neurophysiol 116:2510–2519.

Canolty RT, Soltani M, Dalal SS, Edwards E, Dronkers NF, Nagarajan SS, Kirsch HE, Barbaro NM, Knight RT (2007) Spatiotemporal dynamics of word processing in the human brain. Front Neurosci 1:185–196.

Chambers CD, Garavan H, Bellgrove MA (2009) Insights into the neural basis of response inhibition from cognitive and clinical neuroscience. Neurosci Biobehav Rev 33:631–646.

Chikazoe J (2010) Localizing performance of go/no-go tasks to prefrontal cortical subregions. Curr Opin Psychiatry 23:267–272.

Delorme A, Makeig S (2004) EEGLAB: an open source toolbox for analysis of single-trial EEG dynamics including independent component analysis. J Neurosci Methods 134:9–21.

Eagle DM, Baunez C, Hutcheson DM, Lehmann O, Shah AP, Robbins TW (2008) Stop-signal reaction-time task performance: role of prefrontal cortex and subthalamic nucleus. Cereb Cortex 18:178–188.

Folstein JR, Van Petten C (2008) Influence of cognitive control and mismatch on the N2 component of the ERP: a review. Psychophysiology 45:152–170.

Ford A, McGregor KM, Case K, Crosson B, White KD (2010) Structural connectivity of Broca's area and medial frontal cortex. Neuroimage 52:1230–1237.

Forstmann BU, Anwander A, Schäfer A, Neumann J, Brown S, Wagenmakers EJ, Bogacz R, Turner R (2010) Cortico-striatal connections predict control over speed and accuracy in perceptual decision making. Proc Natl Acad Sci U S A 107:15916–15920.

Garavan H, Ross TJ, Stein EA (1999) Right hemispheric dominance of inhibitory control: an event-related functional MRI study. Proc Natl Acad Sci U S A 96:8301–8306.

Garavan H, Hester R, Murphy K, Fassbender C, Kelly C (2006) Individual differences in the functional neuroanatomy of inhibitory control. Brain Res 1105:130–142.

Garcia-Munoz M, Carrillo-Reid L, Arbuthnott GW (2010) Functional anatomy: dynamic states in basal ganglia circuits. Front Neuroanat 4:144.

Gauggel S, Rieger M, Feghoff TA (2004) Inhibition of ongoing responses in patients with Parkinson's disease. J Neurol Neurosurg Psychiatry 75:539–544.

Goetz CG, Stebbins GT, Chmura TA, Fahn S, Klawans HL, Marsden CD (1995) Teaching tape for the motor section of the unified Parkinson's disease rating scale. Mov Disord 10:263–266.

Hammond C, Bergman H, Brown P (2007) Pathological synchronization in Parkinson's disease: networks, models and treatments. Trends Neurosci 30:357–364.

Hampshire A, Chamberlain SR, Monti MM, Duncan J, Owen AM (2010) The role of the right inferior frontal gyrus: inhibition and attentional control. Neuroimage 50:1313–1319.

Hoehn MM, Yahr MD (1967) Parkinsonism: onset, progression and mortality. Neurology 17:427–442.

Inase M, Tokuno H, Nambu A, Akazawa T, Takada M (1999) Corticostriatal and corticosubthalamic input zones from the presupplementary motor area in the macaque monkey: comparison with the input zones from the supplementary motor area. Brain Res 833:191–201.

Isoda M, Hikosaka O (2008) Role for subthalamic nucleus neurons in switching from automatic to controlled eye movement. J Neurosci 28:7209–7218.

Johansen-Berg H, Behrens TE, Robson MD, Drobnjak I, Rushworth MF, Brady JM, Smith SM, Higham DJ, Matthews PM (2004) Changes in connectivity profiles define functionally distinct regions in human medial frontal cortex. Proc Natl Acad Sci U S A 101:13335–13340.

Jung TP, Makeig S, Westerfield M, Townsend J, Courchesne E, Sejnowski TJ (2000) Removal of eye activity artifacts from visual event-related potentials in normal and clinical subjects. Clin Neurophysiol 111:1745–1758.

Kok A, Ramautar JR, De Ruiter MB, Band GP, Ridderinkhof KR (2004) ERP components associated with successful and unsuccessful stopping in a stop-signal task. Psychophysiology 41:9–20.

Konishi S, Nakajima K, Uchida I, Kikyo H, Kameyama M, Miyashita Y (1999) Common inhibitory mechanism in human inferior prefrontal cortex revealed by event-related functional MRI. Brain 122:981–991.

Kühn AA, Williams D, Kupsch A, Limousin P, Hariz M, Schneider G-H, Yarrow K, Brown P (2004) Event-related beta desynchronization in human subthalamic nucleus correlates with motor performance. Brain 127:735–746.

Kühn AA, Kupsch A, Schneider G-H, Brown P (2006) Reduction in subthalamic 8–35 Hz oscillatory activity correlates with clinical improvement in Parkinson's disease. Eur J Neurosci 23:1956–1960.

Kühn AA, Kempf F, Brücke C, Gaynor Doyle L, Martinez-Torres I, Pogosyan A, Trottenberg T, Kupsch A, Schneider G-H, Hariz MI, Vandenberghe W, Nuttin B, Brown P (2008) High-frequency stimulation of the subthalamic nucleus suppresses oscillatory beta activity in patients with Parkinson's disease in parallel with improvement in motor performance. J Neurosci 28:6165–6173.

Kühn AA, Tsui A, Aziz T, Ray N, Brücke C, Kupsch A, Schneider G-H, Brown P (2009) Pathological synchronisation in the subthalamic nucleus of patients with Parkinson's disease relates to both bradykinesia and rigidity. Exp Neurol 215:380–387.

Kulisevsky J, Berthier ML, Gironell A, Pascual-Sedano B, Molet J, Parés P (2002) Mania following deep brain stimulation for Parkinson's disease. Neurology 59:1421–1424.

Kuncel AM, Grill WM (2004) Selection of stimulus parameters for deep brain stimulation. Clin Neurophysiol 115:2431–2441.

Li CS, Yan P, Sinha R, Lee TW (2008) Subcortical processes of motor response inhibition during a stop signal task. Neuroimage 41:1352–1363.

Liotti M, Pliszka SR, Perez R 3rd, Luus B, Glahn D, Semrud-Clikeman M (2007) Electrophysiological correlates of response inhibition in children and adolescents with ADHD: influence of gender, age, and previous treatment history. Psychophysiology 44:936–948.

Logan GD, Schachar RJ, Tannock R (1997) Impulsivity and inhibitory control. Psychol Sci 8:60–64.

Luck SJ (2005) An introduction to the event-related potential technique. Cambridge, MA: MIT Press.

Mallet L, Schüpbach M, N'Diaye K, Remy P, Bardinet E, Czernecki V, Welter ML, Pelissolo A, Ruberg M, Agid Y, Yelnik J (2007) Stimulation of subterritories of the subthalamic nucleus reveals its role in the integration of the emotional and motor aspects of behavior. Proc Natl Acad Sci U S A 104:10661–10666.

Marco-Pallarés J, Camara E, Münte TF, Rodríguez-Fornells A (2008) Neural mechanisms underlying adaptive actions after slips. J Cogn Neurosci 20:1595–1610.

Neubert FX, Mars RB, Buch ER, Olivier E, Rushworth MF (2010) Cortical and subcortical interactions during action reprogramming and their related white matter pathways. Proc Natl Acad Sci U S A 107:13240–13245.

Pliszka SR, Liotti M, Woldorff MG (2000) Inhibitory control in children with attention-deficit/hyperactivity disorder: event-related potentials identify the processing component and timing of an impaired right-frontal response-inhibition mechanism. Biol Psychiatry 48:238–246.

Pogosyan A, Gaynor LD, Eusebio A, Brown P (2009) Boosting cortical activity at beta-band frequencies slows movement in humans. Curr Biol 19:1637–1641.

Ramautar JR, Kok A, Ridderinkhof KR (2006) Effects of stop-signal modality on the N2/P3 complex elicited in the stop-signal paradigm. Biol Psychol 72:96–109.

Ray N, Jenkinson N, Brittain J, Holland P, Joint C, Nandi D, Bain P, Yousif N, Green A, Stein J, Aziz T (2009) The role of the subthalamic nucleus in response inhibition: evidence from deep brain stimulation for Parkinson's disease. Neuropsychologia.

Rieger M, Gauggel S, Burmeister K (2003) Inhibition of ongoing responses following frontal, nonfrontal, and basal ganglia lesions. Neuropsychology 17:272–282.

Rubia K, Smith AB, Brammer MJ, Taylor E (2003) Right inferior prefrontal cortex mediates response inhibition while mesial prefrontal cortex is responsible for error detection. Neuroimage 20:351–358.

Schmajuk M, Liotti M, Busse L, Woldorff MG (2006) Electrophysiological activity underlying inhibitory control processes in normal adults. Neuropsychologia 44:384–395.

Sharp DJ, Bonnelle V, De Boissezon X, Beckmann CF, James SG, Patel MC,

Mehta MA (2010) Distinct frontal systems for response inhibition, attentional capture, and error processing. Proc Natl Acad Sci U S A 107: 6106–6111.

Swann N, Tandon N, Canolty R, Ellmore TM, McEvoy LK, Dreyer S, DiSano M, Aron AR (2009) Intracranial EEG reveals a time- and frequency-specific role for the right inferior frontal gyrus and primary motor cortex in stopping initiated responses. J Neurosci 29:12675–12685.

Temperli P, Ghika J, Villemure J-G, Burkhard PR, Bogousslavsky J, Vingerhoets FJG (2003) How do parkinsonian signs return after discontinuation of subthalamic DBS? Neurology 60:78–81.

van den Wildenberg WPM, van Boxtel GJM, van der Molen MW, Bosch DA, Speelman JD, Brunia CHM (2006) Stimulation of the subthalamic region facilitates the selection and inhibition of motor responses in Parkinson's disease. J Cogn Neurosci 18:626–636.

Verbruggen F, Logan GD (2009a) Models of response inhibition in the stop-signal and stop-change paradigms. Neurosci Biobehav Rev 33:647–661.

Verbruggen F, Logan GD (2009b) Proactive adjustments of response strategies in the stop-signal paradigm. J Exp Psychol Hum Percept Perform 35:835–854.

Verbruggen F, Aron AR, Stevens MA, Chambers CD (2010) Theta burst stimulation dissociates attention and action updating in human inferior frontal cortex. Proc Natl Acad Sci U S A 107:13966–13971.

Wingeier B, Tcheng T, Koop MM, Hill BC, Heit G, Bronte-Stewart HM (2006) Intra-operative STN DBS attenuates the prominent beta rhythm in the STN in Parkinson's disease. Exp Neurol 197:244–251.